An Impedance Based Fault Location Algorithm for Tapped Lines Using Local Measurements

Ahad Esmaeilian, Student Member, IEEE, and Mladen Kezunovic, Fellow, IEEE
Department of Electrical and Computer Engineering, Texas A&M University
College Station, Texas, 77843, USA
Emails: ahadesmaeilian@tamu.edu ; kezunov@ee.tamu.edu

***Abstract*— The tapped lines are usually used to supply a customer such as small communities or industrial facilities with an economic solution that is less expensive than building a full substation. Locating faults in such lines are difficult due to the effect of infeed/outfeed current from tapped lines as well as reactance effect. The proposed method applies generalized models of fault loop voltage and current to formulate the fault location algorithm. The derived algorithm has a very simple first-order formula and does not require knowledge of data from the other ends. This feature becomes more significant in the case of isolated rural areas where communicational link to exchange data with other ends may not exist. The result of the algorithm performance evaluation using simulations verifies the high accuracy of the method with regard to various equivalent source impedances, fault inception angles, fault resistances and locations as well as fault types.**

I. INTRODUCTION

In some situations of serving loads or integrating wind or solar generation, customers are connected to an existing transmission line using a tapped line because of economic advantages. Such a configuration of transmission lines presents great difficulty for the task of fault location because measurements from the tapped line end may not be readily available [1].

So far, different fault location algorithms for three-terminal transmission lines have been developed [2]–[14]. Several algorithms known as one-ended fault location techniques assume the data to be available at local terminal [2]-[4]. Many other algorithms use data from more than one terminal.

In [5] synchronized voltage and current waveforms measured at all three terminals are used to calculate the fault location. The authors utilized the prefault measurements at three terminals to synchronize the waveforms. An alternative approach is presented in [6], which similarly uses measurements from all three terminals of the transmission line but does not require synchronized data from all terminals. Employing an iterative algorithm, the synchronization error is estimated and the fault location is obtained. In [7]-[8] authors used synchronized three-phase voltages and currents at all terminals. In [8] they proposed an algorithm which applies voltage differentials at terminals to gradually reduce a multi-terminal line to a two-terminal line containing the faulted section. Then, a reactive power-based method was employed to locate the fault.

In [9] authors use current differentials at terminals to perform a similar reduction. The reduction procedure is very complicated and also normalizes section impedances when impedances are different. Exchanging the minimal amount of information between the line terminals is considered in [10]-[12]. The use of negative-sequence quantities for fault location in three-terminal lines, which uses magnitude of negative-sequence current as well as the negative-sequence source impedance of remote terminals, is proposed in [10]. The technique introduced in [11], only utilizes voltage signals for the fault location, so it is immune to current transformer saturation. In [12], complete measurement from one end with supplementary information of load currents from the two remote ends is considered.

The fault location becomes quite challenging in the case of tapped lines because exchanging synchronized or even unsynchronized data through proper communicational links may not be possible. In [13], a PMU based algorithm using synchronized measurements from two ends of the transmission line is proposed. This algorithm, first, estimates the equivalent source impedances, and then the fault location is calculated by taking the effect of infeed current into account. Although this algorithm does not require any information from the tapped line, change of the equivalent source impedance, that is likely in power networks, could significantly affect the calculated distance to fault point.

Another approach for locating faults on overhead transmission lines is known as traveling-wave based technique which utilizes the high frequency components of the fault generated transients [14]-[15]. The algorithm proposed in [14] detects the arrival times of fault initiated traveling-waves reflected from the discontinuities by use of Wavelet transform. Although the algorithm does not depend on fault type, fault resistance and mutual coupling between the lines, the accuracy of the algorithm accuracy is proportional to the sampling frequency. Similarly, the accuracy of the algorithm proposed in [15] depends on the sampling frequency and would be affected by an increase in the noise ratio. These methods could provide more accurate results, but are more complex and costly for practical application compared to power frequency based techniques.

This paper presents a new impedance based fault location algorithm which utilizes just local voltages and currents measurements at one end of the transmission line. The proposed algorithm is discussed in section II, the simulation study results are presented in section II and conclusion are outlined in section IV.

II. PROPOSED FAULT LOCATION ALGORITHM

The proposed algorithm in this study estimates the distance to fault independent of the infeed/outfeed current from the other two terminals and fault path resistance. For the three-terminal transmission line as shown in Fig. 1, it is assumed that the sampled data of the voltages and line currents is available at terminal A. The algorithm utilizes the fundamental components of the voltage and current measured at bus A to locate faults at the three legs of a typical tapped transmission line.

Fault loop voltage and current measured at bus A can be expressed in terms of symmetrical components by using the coefficients a_0 , a_1 , a_2 gathered in Table I [16], as below equations:

$$V_{A\varphi} = a_1 V_{A1} + a_2 V_{A2} + a_0 V_{A0} \quad (1)$$

$$I_{A\varphi} = a_1 I_{A1} + a_2 I_{A2} + a_0 \frac{Z_{0L}}{Z_{1L}} I_{A0} \quad (2)$$

where 0, 1 and 2 indicate the zero, positive and negative sequences and φ=a,b,c indicate each three phases.

On the other hand, regardless of the fault type, the fault current can be expressed as:

$$I_f = C_1 I_{f1} + C_2 I_{f2} + C_0 I_{f0} \quad (3)$$

where I_{f1}, I_{f2} and I_{f0} are the positive-, negative- and zero-sequence components of the fault current and C_1, C_2 and C_0 are the current weight coefficients for positive, negative and zero sequence components.

These coefficients can be determined by considering the boundary conditions for a particular fault type. When the fault location is close to the remote ends of the transmission line, the phase-angle of C_0 would be too large which affects the accuracy of the estimated fault distance. But there is some freedom in fault current weight coefficients determination. In fact, it is possible to eliminate the zero-sequence coefficient to avoid above mentioned problem. Table II shows the fault current weight coefficients [15]. After setting $C_0 = 0$ (as in Table 2) only the positive and the negative sequence components of the total fault current shall be determined.

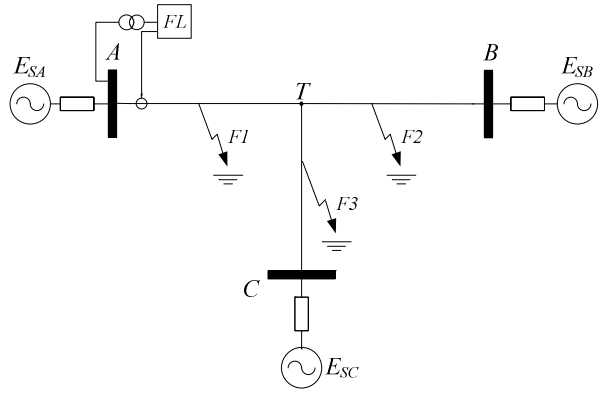

Figure 1. A typical three-terminal transmission line.

TABLE I. SHARE COEFFICIENTS USED FOR DETERMINING FAULT LOOP SIGNALS.

Fault type	a_1	a_2	a_0
a-g	1	1	1
b-g	α^2	α	1
c-g	α	α^2	1
a-b, a-b-g, a-b-c, a-b-c-g	$1-\alpha^2$	$1-\alpha$	0
b-c, b-c-g	α^2-1	$\alpha-\alpha^2$	0
c-a, c-a-g	$\alpha-1$	α^2-1	0
$\alpha=\exp(j2\pi/3)$			

TABLE II. FAULT CURRENT WEIGHTING COEFFICIENTS

Fault type	C_1	C_2	C_0
a-g	3	0	0
b-g	$3\alpha^2$	0	0
c-g	3α	0	0
a-b	$1-\alpha^2$	0	0
b-c	$\alpha^2-\alpha$	0	0
c-a	$\alpha-1$	0	0
a-b-g	$1-\alpha^2$	$1-\alpha$	0
b-c-g	$\alpha^2-\alpha$	$\alpha-\alpha^2$	0
c-a-g	$\alpha-1$	α^2-1	0
a-b-c-g	$1-\alpha^2$	0	0
$\alpha=\exp(j2\pi/3)$			

These coefficients will be used in next subsections to calculate the current distribution factor for the purpose of eliminating the effect of infeed/outfeed current as well as reactance effect on the algorithm.

For ease of description, the proposed algorithm is derived based on $V_{A\varphi}$ and $I_{A\varphi}$ calculated from (1) and (2). While for each fault type the fault loop voltage and current measured at bus A can be obtained by substituting the proper share coefficients from Table I.

To establish the fault location scheme, the algorithm is divided into three subroutines each related to one section. (See Fig. 1). The next subsections describe each subroutine.

A. Section A-T subroutine

According to Fig. 2 the generalized fault loop voltage measured at bus A where the fault locator is installed for a fault occurred in section A-T is obtain from (4).

$$V_{A\varphi} - d_1 . Z_{LA} . I_{A\varphi} - R_f . (C_1 . I_{f1} + C_2 . I_{f2}) = 0 \quad (4)$$

Unknown values I_{f1} and I_{f2} can be derived from equivalent circuit diagrams for positive and negative sequences shown in Fig. 2. The equations resulting from the equivalent circuit diagrams are as follows:

$$I_{f1} = \frac{\Delta I_{A1}}{k_f} \quad , \quad I_{f2} = \frac{I_{A2}}{k_f} \quad (5)$$

where ΔI_{A1} is the superimposed positive sequence current, I_{A2} is the negative sequence current and k_f is the current distribution factor which is identical for the positive and negative sequences.

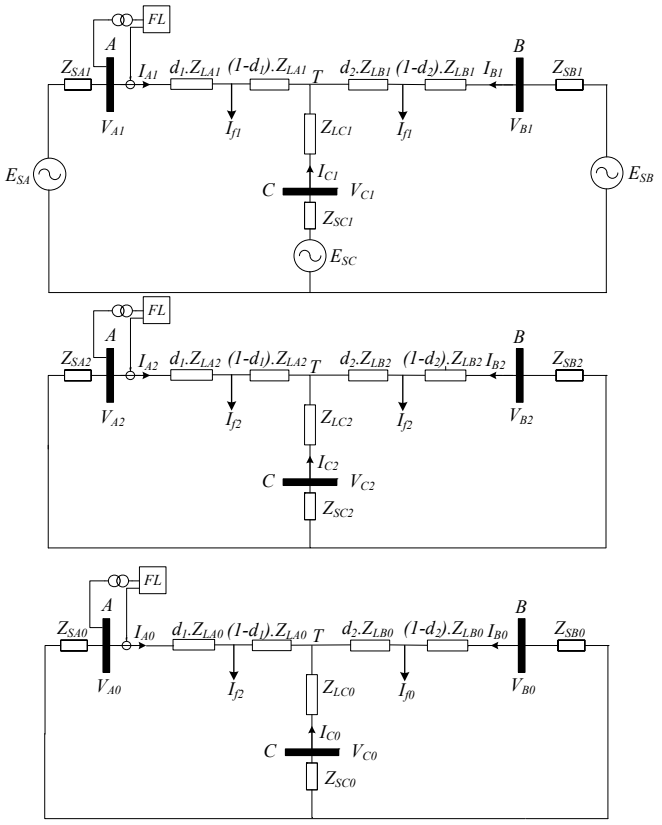

Figure 2. Positive, negative and zero sequence diagram for fault in section A-T or T-B.

From Fig. 2, by applying two KVL equations for each sequence, after simplification the current distribution factor is obtained as below:

$$k_f = \frac{K_1 + L_1.d_1}{M_1} \tag{6}$$

where:

$$K_1 = (Z_{SC} + Z_{LC}).(Z_{SB} + Z_{LB})$$

$$L_1 = -Z_{LB}.(Z_{SC} + Z_{LC})$$

$$M_1 = (Z_{SA} + Z_{LA}).(Z_{SC} + Z_{LC}) + (Z_{SA} + Z_{LA}).(Z_{SB} + Z_{LB}) + (Z_{SB} + Z_{LB}).(Z_{SC} + Z_{LC})$$

Equation (6) indicates that the current distribution factor is a function of an unknown distance to fault (d, [p.u.]) as well as source impedances Z_{SA}, Z_{SB} and Z_{SC} .It will be further shown that it is not necessary to determine the value of k_f .

From (5) the total fault current can be rewritten as:

$$I_f = \frac{(C_1.\Delta I_{A1} + C_2.I_{A2})}{k_f} \tag{7}$$

In general, the current distribution factor is a complex number and it may be presented as $k_f = K_F.e^{j\gamma}$. However, as illustrated in simulation results, γ is close to zero. So, k_f can be considered as real coefficient. By substituting K_F into equation (4) and dividing it by $I_{A\varphi}$ one can obtain:

$$Z_{A\varphi} - d_1.Z_{LA} - \frac{R_f}{K_F}.\beta_{12} = 0 \tag{8}$$

where:

$$\beta_{12} = \frac{(C_1.\Delta I_{A1} + C_2.I_{A2})}{I_{A\varphi}}$$

Resolving (8) into real and imaginary parts gives:

$$R_{A\varphi} - d_1.R_{LA} - \frac{R_f}{K_F}.\mathrm{Re}\{\beta_{12}\} = 0 \tag{9}$$

$$X_{A\varphi} - d_1.X_{LA} - \frac{R_f}{K_F}.\mathrm{Im}\{\beta_{12}\} = 0 \tag{10}$$

Elimination of the term R_f/K_F yields the following formula for a sought distance to fault:

$$d_1 = \frac{\mathrm{Im}\{\beta_{12}\}.R_{A\varphi} - \mathrm{Re}\{\beta_{12}\}.X_{A\varphi}}{\mathrm{Im}\{\beta_{12}\}.R_{LA} - \mathrm{Re}\{\beta_{12}\}.X_{LA}} \tag{11}$$

The formula (11) can be written in a more compact form:

$$d_1 = \frac{\mathrm{Im}\{Z_{A\varphi}.\beta_{12}^*\}}{\mathrm{Im}\{Z_{LA}.\beta_{12}^*\}} \tag{12}$$

where β_{12}^* is the conjugate of β_{12} . So the distance measured by fault locator from fault point to bus A can be expressed as:

$$d = L_{AT}.d_1 \tag{13}$$

where L_{AT} denote the length of the section A-T.

B. Section T-B subroutine

Referring to Fig. 2, for a fault occurring at an arbitrary distance d_2 from T point in the section T-B, the voltage measured by the relay at bus A is respectively given by:

$$V_{A\varphi} - Z_{LA}.I_{A\varphi} - d_2.Z_{LB}.(I_{A\varphi} + I_{C\varphi}) - R_f.I_f = 0 \tag{14}$$

Reffering to Fig. 2 and (2), $I_{C\varphi}$ can be written as a function of $I_{A\varphi}$ through below calculations:

$$\frac{I_{C\varphi}}{I_{A\varphi}} = \frac{a_1(\frac{E_C - E_A}{Z_C'} + \frac{Z_A'}{Z_C'}I_{A1}) + a_2\frac{Z_A'}{Z_C'}I_{A2} + a_0'\frac{Z_A'}{Z_C'}I_{A0}}{I_{A\varphi} = a_1I_{A1} + a_2I_{A2} + a_0'I_{A0}} \tag{15}$$

where:

$$a_0' = a_0\frac{Z_{0L}}{Z_{1L}} \quad , \quad \frac{Z_A'}{Z_C'} = \frac{Z_{SA} + Z_{LA}}{Z_{SC} + Z_{LC}}$$

Then, (15) can be rewritten as (16).

$$I_{C\varphi} = a_1.\frac{E_C - E_A}{Z_C'} + \frac{Z_A'}{Z_C'}I_{A\varphi} \tag{16}$$

According to simulation results presented in next section, neglecting the first term in right hand side of the equation (16) is permissible due to its inconsequential value. So the relation between $I_{A\varphi}$ and $I_{C\varphi}$ is simplified as equation (17).

$$I_{C\varphi} = \frac{Z_A'}{Z_C'}.I_{A\varphi} = \rho_1.I_{A\varphi} \tag{17}$$

Equation (17) indicates a linear, constant relation between $I_{A\varphi}$ and $I_{C\varphi}$. By substituting (17) into (14) and dividing it by $I_{A\varphi}$, Similar to previous subroutine, one can obtain:

$$Z_{A\varphi} - Z_{LA} - d_2.Z_{LB}.(1+\rho_1) - \frac{R_f}{K_F}.\beta_{12} = 0 \qquad (18)$$

Resolving (18) into real and imaginary parts, eliminating the agent R_f/K_F and writing a compact form yields the following equation:

$$d_2 = \frac{\mathrm{Im}\{[Z_{A\varphi} - Z_{LA}].\beta_{12}^*\}}{\mathrm{Im}\{Z_{LB}.(1+\rho_1).\beta_{12}^*\}} \qquad (19)$$

Therefore, the distance between the fault point and bus A is given by:

$$d = L_{AT}.(1+\frac{L_{TB}}{L_{AT}}.d_2) \qquad (20)$$

where L_{AT} and L_{TB} denote the length of the section A-T and the section T-B, respectively.

C. Section T-C subroutine

Referring to Fig. 3, for a fault occurring at an arbitrary distance d_3 from point T in the section T-C, the voltage measured by the relay at bus A is respectively given by:

$$V_{A\varphi} - Z_{LA}.I_{A\varphi} - d_3.Z_{LC}.(I_{A\varphi} + I_{B\varphi}) - R_f.I_f = 0 \qquad (21)$$

As shown in previous subsection, $I_{B\varphi}$ can be written as a function of $I_{A\varphi}$ similar to (17).

$$I_{C\varphi} = \frac{Z_{SA} + Z_{LA}}{Z_{SB} + Z_{LB}}.I_{A\varphi} = \rho_2.I_{A\varphi} \qquad (22)$$

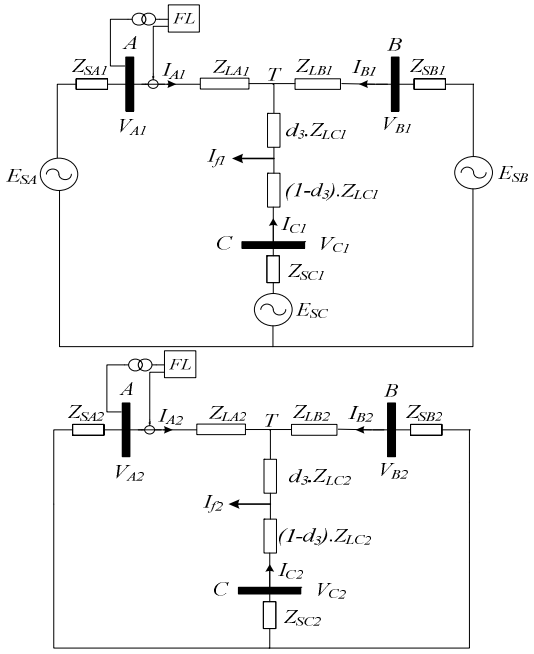

Figure 3. Positive and negative sequence diagram for fault in section T-C.

Taking into account equations (8) and (22), the equation below can be obtained from (21).

$$Z_{A\varphi} - Z_{LA} - d_3.Z_{LC}.(1+\rho_2) - \frac{R_f}{K_F}.\beta_{12} = 0 \qquad (23)$$

Resolving (23) into real and imaginary parts, eliminating the term R_f/K_F and writing a compact form yields the following equation:

$$d_3 = \frac{\mathrm{Im}\{[Z_{A\varphi} - Z_{LA}].\beta_{12}^*\}}{\mathrm{Im}\{Z_{LC}.(1+\rho_2).\beta_{12}^*\}} \qquad (24)$$

Therefore, the distance between the fault point and bus A is given by:

$$d = L_{AT}.(1+\frac{L_{TC}}{L_{AT}}.d_3) \qquad (25)$$

where L_{TC} denote the length of the section T-C.

III. Simulation Study

This section describes the results acquired by the proposed algorithm and its performance when it is subjected to different test conditions.

A. Simulated Model

For more accurate results, the distributed model of transmission line is used in the performed simulation. The modeled 230kV test network includes the line sections–A-T: 100 km, T-B: 90 km, T-C: 70 km, having the positive-(negative-) and zero-sequence impedances:

$$Z_{LA}^1 = Z_{LA}^2 = Z_{LB}^1 = Z_{LB}^2 = Z_{LC}^1 = Z_{LC}^2 = 0.034 + j0.419\Omega/km$$

$$Z_{LA}^0 = Z_{LB}^0 = Z_{LC}^0 = 0.291 + j1.157\Omega/km$$

The equivalent source impedances:

$$Z_{SA} = 1.23 + j16.5\Omega \quad , \quad Z_{SB} = Z_{SA} \quad , \quad Z_{SC}^0 = 1.5Z_{SA}$$

were also included. The prefault load flow in the modeled network is controlled by the assumed phase shift of side B source (i.e. -25°) and side C source (i.e. -15°), with respect to the bus A source (0°).

B. Evaluation of Transient Response

In order to verify and evaluate the proposed fault location algorithm different scenarios are taken into account. Three fault scenarios with different fault types, resistance values and locations along the three legs of the modeled transmission line are simulated.

In the first case, an a-g fault at 170km from the relay point, at section T-B, with 20Ω resistance is considered to occur at t=0.3 sec. Fig. 4 shows the related distance to fault measured by the algorithm. It is obvious that the transients are rapidly damped and the algorithm has an accurate result in this case.

In the second case, an ab-g fault at 20km from the relay point, at section A-T, with 50Ω resistance is considered. Fig. 5 shows the relative fault location result. In this case also the oscillations are damped very fast (less than 0.5 sec).

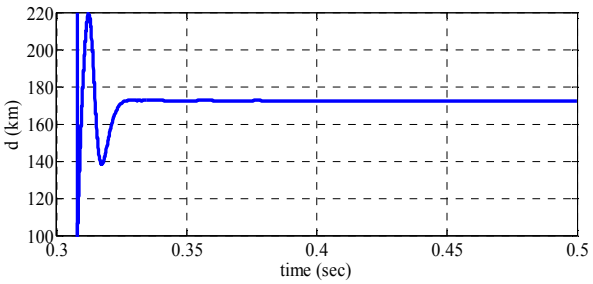

Figure 4. a-g fault with 20Ω resistance 170km from bus A at section B-T.

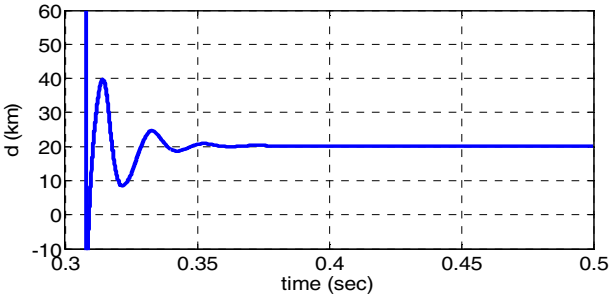

Figure 5. ab-g fault with 50Ω resistance 20km from bus A at section A-T.

C. *Evaluation of Steady-State Error*

Steady-state errors of the measured distance from relay to fault point are studied in this subsection for different fault location, fault path resistance, fault type, location of tapped line, tapped load condition and fault inception angle. The percentage errors shown in the following figures are calculated by equation from IEEE PC37.114:

$$\%Error = \frac{(d_{measured} - d_{actual})}{d_{total}} \times 100$$

Fig. 6 presents the estimated fault location errors for a c-g fault when the fault is moved from bus A to bus B by 5km intervals for three different fault resistances. In the worst case, when fault occurs at bus B with 100Ω, the error does not exceed 1.2 %. It should be noticed that the error increases when the fault occurs near the tapped point. Fig. 7 also shows the estimated fault location errors versus the distance to fault point for an abc-g fault. The fault point changes from relay point at bus A to Bus C across the sections A-T and T-C. In the worst case, when the fault occurs at bus C with 50Ω, the error does not exceed 0.8 %.

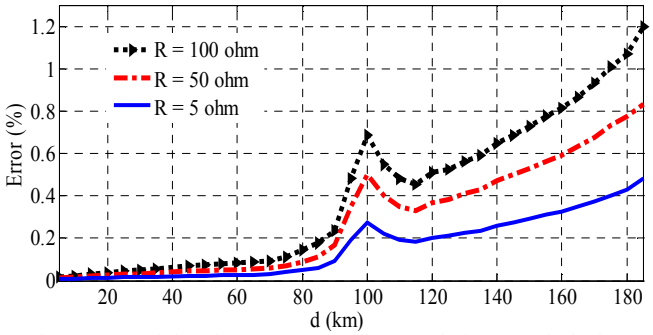

Figure 6. Fault location error versus distance, during a c-g fault along sections A-T and T-B for three different fault resistances.

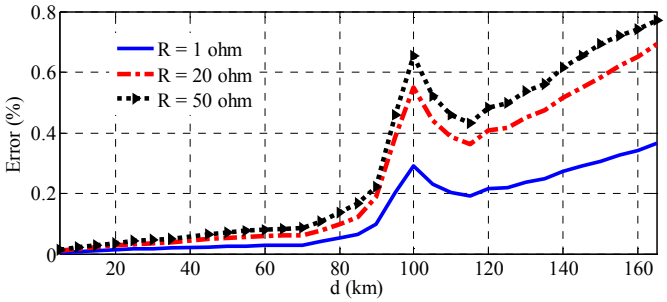

Figure 7. Fault location error versus distance, during an abc-g fault along sections A-T and T-C for three different fault resistances.

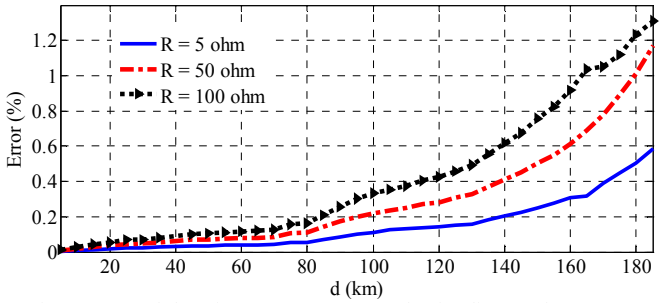

Figure 8. Fault location error versus tapped point distance from Bus A during an ac-g fault at the middle point of section T-C for three different fault resistances.

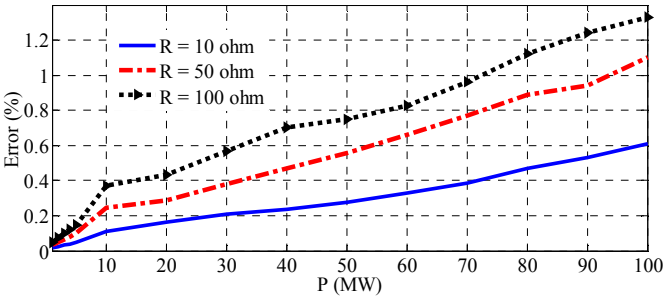

Figure 9. Fault location error versus tapped end (bus C) active power during an a-g fault at the middle point of section T-B for three different fault resistances.

To investigate the effect of tapped point location, the T point location is changed between the bus A and C with 5km intervals. The fault location error for three different fault path resistances is shown in Fig. 8. In the worst case, when the tapped point is located near the bus B and the fault resistance is considered to be 100Ω, the related error is less than 1.3 %.

In order to investigate influence of the tapped line loading condition on the proposed algorithm performance, some further simulations were performed. Fig. 9 depicts the fault location algorithm errors versus active power measured at bus C for an a-g fault in the middle point of section T-C for three different fault resistances. As can be seen, the fault location estimation error increases by increase of the tapped line power flow. Nevertheless, in the worst case, the error is less than 1.4%.

Table III also shows supplimentary tests condition and related fault location errors. Different fault inception angles, fault type and fault distance from bus A are considered. The results indicate that in the worst case the fault location error does not exceed 0.9 %.

TABLE III. FAULT DISTANCE ESTIMATION WITH REGARD TO CHANGING FAULT DISTANCE, FAULT TYPE AND FAULT INCEPTION ANGLE

Fault distance from bus A (km)	Fault inception angle (°)	Fault type	Fault location error (%)
5	30	a-g	0.011
20	45	b-g	0.032
40	0	a-b	0.056
70	60	abc-g	0.095
100	120	c-g	0.243
140	135	bc-g	0.379
160	160	b-c	0.582
180	90	abc	0.876

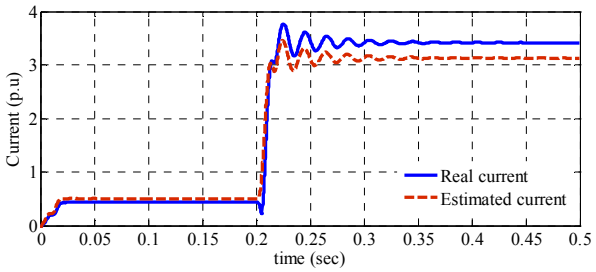

Figure 10. Effect of source impedance variation on current estimation.

D. *Effect of Source impedance*

In this subsection the effect of source impedance on the accuracy of the proposed fault location algorithm is taken into consideration. This study demonstrates that, irrespective the fact that the algorithm utilizes the equivalent source impedance to estimate the current from the other ends of transmission line, the effect of equivalent source is small enough to be neglected. The equivalent source impedance may change during different seasons or as consequences of nearby transmission lines outage. Due to the robustness of the algorithm, despite the change in the equivalent source impedance of bus A and B increased from 1 pu to 1.2 pu and the equivalent source impedance of bus C decreased from 1.5 pu to 1.2 pu, the algorithm demonstrates high accuracy. Fig. 10 shows the estimation of $I_{C\varphi}$ using (17), when a single phase to ground fault with fault resistance R_f=10Ω located at the middle of section T-C is occurred at t=0.2sec. It should be noticed that the algorithm uses the old values of equivalent source impedances to estimate $I_{C\varphi}$ as well as location of fault. The results indicate that the effect of source impedance change is still negligible. In the worst case, the error in the final calculated distance to fault caused by these changes does not exceed from 3 %.

IV. CONCLUSION

This study proposes a new fault location algorithm for the tapped transmission lines which utilizes only local voltages and currents. The following are the contributions of the work reported in this paper:

- Detailed impedance of the network has to be provided as the input data to the algorithm. The algorithm considers the effect of fault resistance as well as infeed/outfeed current by defining current distribution factor and estimating current from the other ends.
- Determining the fault point based on the first order formula calculation shows the simplicity and great computational advantage of the method over the ones introduced in the past.
- Large variety of simulation studies have been carried out to corroborate the operation of the proposed fault location method when applied to the tapped lines. The maximum error is consistently less than 3 %.
- Effect of different condition such as fault impedance, fault inception angle, fault location, source impedance, location of tapped line and pre fault load condition are eliminated
- The method is based on the symmetrical components approach and thus is intended for application to the transposed lines.

REFERENCES

[1] R. Perera, B. Kasztenny, "Application considerations when protecting lines with tapped and in-line transformers," *Western Protective Relay Conference*, Washington, Apr. 2012.

[2] T. Tagaki, et al., "Development of new type fault locator using the one-terminal voltage and current data," *IEEE Transactions on Power Apparatus and Systems*, vol. PAS-101, no. 8, 1982, pp. 2892-2898.

[3] A. A. Girgis, "A new kalman filtering-based digital distance relay," *IEEE Transactions on Power Apparatus and Systems*, vol. PAS-101, no. 9, August 1982, pp. 3471-3479.

[4] K. Srinvsansan, A. St. Jacques, "A new fault location algorithm for radial transmission lines with loads," *IEEE Transactions on Power Apparatus and Systems*, vol. 4, No. 3, July 1989, pp. 1676-1682.

[5] R.K. Aggarwal, D.V. Coury, A.T. Johns, A. Kalam, "A practical approach to accurate fault location on extra high voltage teed feeders", *IEEE Trans. Power Delivery*, vol. 8, no. 3, pp. 874–883, Jul. 1993.

[6] A. A. Girgis, D.G. Hart, W.L. Peterson, "A new fault location technique for two-and three-terminal lines", *IEEE Trans. Power Delivery*, vol. 7, no. 1, pp. 98–107, Jan. 1992.

[7] A. Esmaeilian, et al., "A precise PMU based fault location method for multi terminal transmission line using voltage and current measurement," *10th International Conference on Environment and Electrical Engineering (EEEIC2011),* 8-11 May, 2011.

[8] M. Abe, et al., "Development of a new fault location system for multi-terminal single transmission lines," *IEEE Trans. Power Del.*, vol. 10, no. 1, pp. 159–168, Jan. 1995.

[9] T. Nagasawa, M. Abe, N. Otsuzuki, T. Emura, Y. Jikihara, and M. Takeuchi, "Development of a new fault location algorithm for multi-terminal two parallel transmission lines," IEEE Trans. Power Del., vol. 7, no. 3, pp. 1516–1532, Jul. 1992.

[10] A. Tziouvaras, J. Roberts, G. Benmmouyal, "New multi-ended fault location design for two or three-terminal lines", 7th Int. IEE Conf. on Developments in Power Sys. Protection, pp. 395–398, Apr. 2001.

[11] S.M. Brahma, "Fault Location scheme for a multi-terminal transmission line using synchronized voltage measurements", *IEEE Trans. on Power Delivery*, vol. 20, no. 2, pp. 1325–1331, Apr. 2005.

[12] J. Izykowski, R. Molag, E. Rosolowski and M.M. Saha, "Fault location in three-terminal line with use of limited measurements," *CD Proceedings of Power Tech, St. Petersburg*, June 2005.

[13] Y. Lin, C. Liu, C. Yu, "New fault locator for three-terminal transmission lines using two-terminal synchronized voltage and current phasors", *IEEE Trans. Power Delivery*, vol. 7, no.3, pp. 452- 459, Jul. 2002.

[14] C. Y. Evrenosoglu, A. Abur, "Travelling wave based fault location for teed circuit," *IEEE Trans. Power Delivery*, vol. 20, no. 2, pp. 1115-1121, April 2005.

[15] M. da Silva, M. Oleskovicz, D. V. Coury, "A fault locator for three-terminal lines based on wavelet transform applied to synchronized current and voltage signals," *TDC '06. IEEE/PES*, pp. 1-6, Aug. 2006.

[16] J. Izykowski, et al., "A new fault location method for application with current differential relays of three terminal lines," *IEEE Trans. Power Delivery*, vol. 22, no.4, pp. 2099- 2107, Oct. 2007.